Table S1. Details of primer sequences used for amplification and targeted replacement of the UDP-galactopyranose mutase-encoding gene *glfA*. Sequences in bold are the reverse complement of the M13R/M13F overlap.

Product	**Primer**	**Sequence 5'→3'**
LF	glf50.1F	TCGCTAAGCTGCGGAGCGCATAGA
	glf50.1R	**GTCGTGACTGGGAAAACCCTGGCG**CCTGCCTTGTAGGATATCCTGGAA
RF	glf30.1F	**TCCTGTGTGAAATTGTTATCCGCT**AATGTTCCTTTCTCATGTACCACG
	glf30.1R	TCGCCCCTGGACGCGTGTTGCTCA
HY	HY split	GGATGCCTCCGCTCGAAGTA
	M13F	CGCCAGGGTTTTCCCAGTCACGAC
YG	YG split	CGTTGCAAGACCTGCCTGAA
	M13R	AGCGGATAACAATTTCACACAGGA
LFHY	glf50.4F	GTATCATCTTGTGATCCGCAAAGG
	HY split	GGATGCCTCCGCTCGAAGTA
RFYG	glf30.1R	TCGCCCCTGGACGCGTGTTGCTCA
	nested YG split	CGCAAGGAATCGGTCAATACACTA
glfA ORF	PROBEF	ATTGGTGCCGGACCTACTGGTCTT
	PROBER	ACAGCTGCTTGGTGAGACCAACGA

Supplementary figures and legends

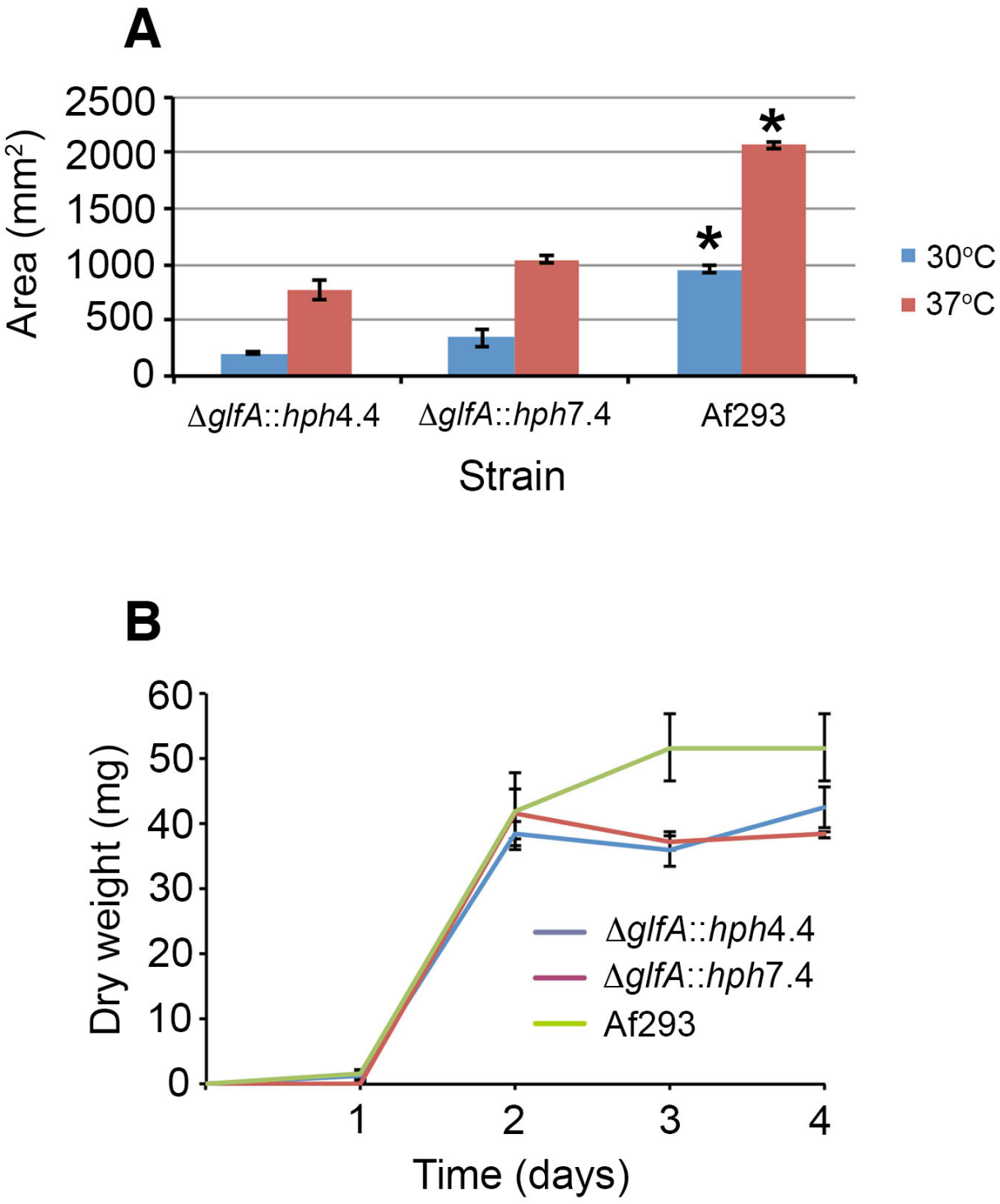

Supplementary Figure 1. A. Colony areas of wild-type Af293 and mutant *A. fumigatus* strains following 3 days growth on MEA at 30 ºC and 37 ºC. Each bar is the mean of 3 replicates ± standard errors, and asterisks by Af293 bars denote significant differences ($P < 0.05$) in mean areas compared to mutant strains at the two different temperatures. Note the

reductions in growth of the two mutant strains at both temperatures when compared to Af293. **B.** Biomass dry weights in mg of mutant and wild-type strains (n=3) over 4 days growth in MEB shake cultures. The growth of all three strains was similar on days 1 and 2, with no additional growth of the two mutants compared to Af293 thereafter. Culture filtrates were tested in ELISA for reactivity with mAbs mJF5 and hJF5 (see Fig 2B).

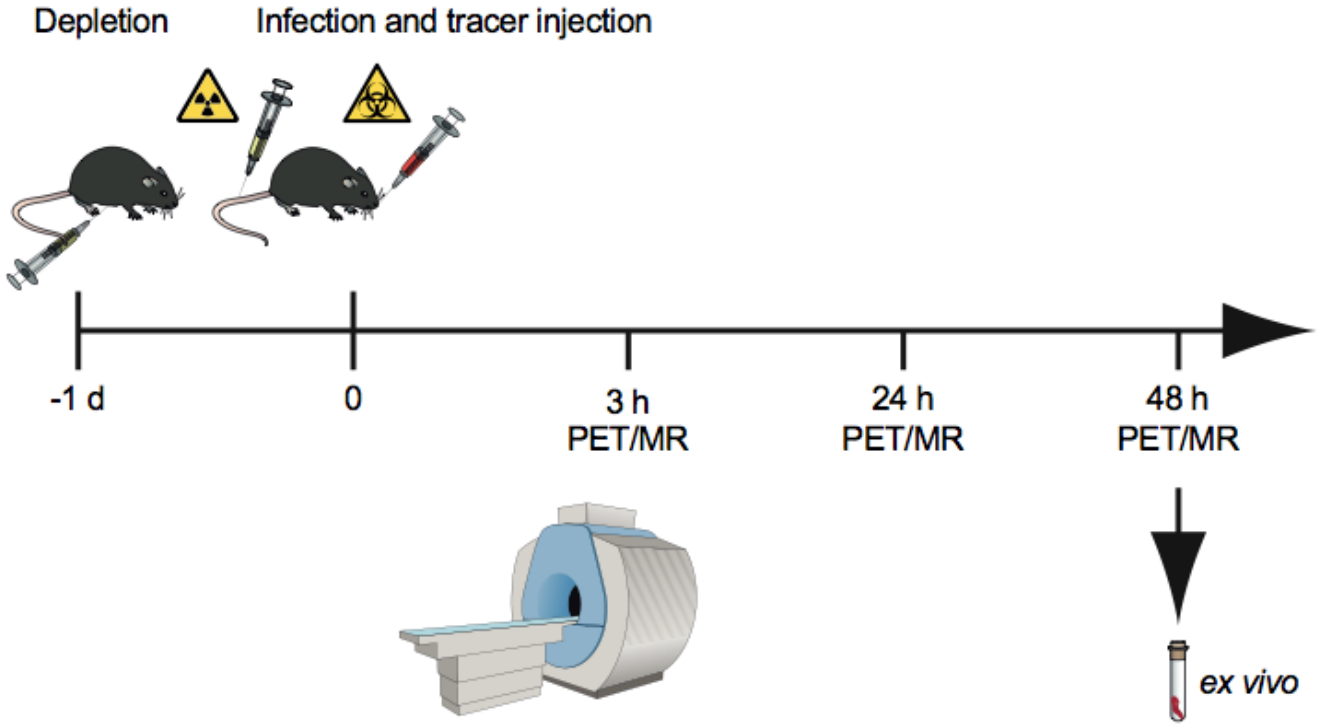

Supplementary Figure 2. Schematic representation of the imaging procedure. 24 h prior to the infection procedure with *A. fumigatus*, neutropenia was induced by the injection of 100 µg per animal of the anti-Ly-6G/anti-Ly6C antibody RB6-8C5. 24 h later, mice were *i.t.* infected with an *A. fumigatus* spore solution for pulmonary fungal infection and the respective PET tracers were *i.v.* injected at the same time. Simultaneous PET/MR imaging of the animals was performed 3 h, 24 h and 48 h after the infection/tracer injection. *Ex vivo* biodistribution and autoradiography were conducted after the last PET scan at 48 h *p.i.*

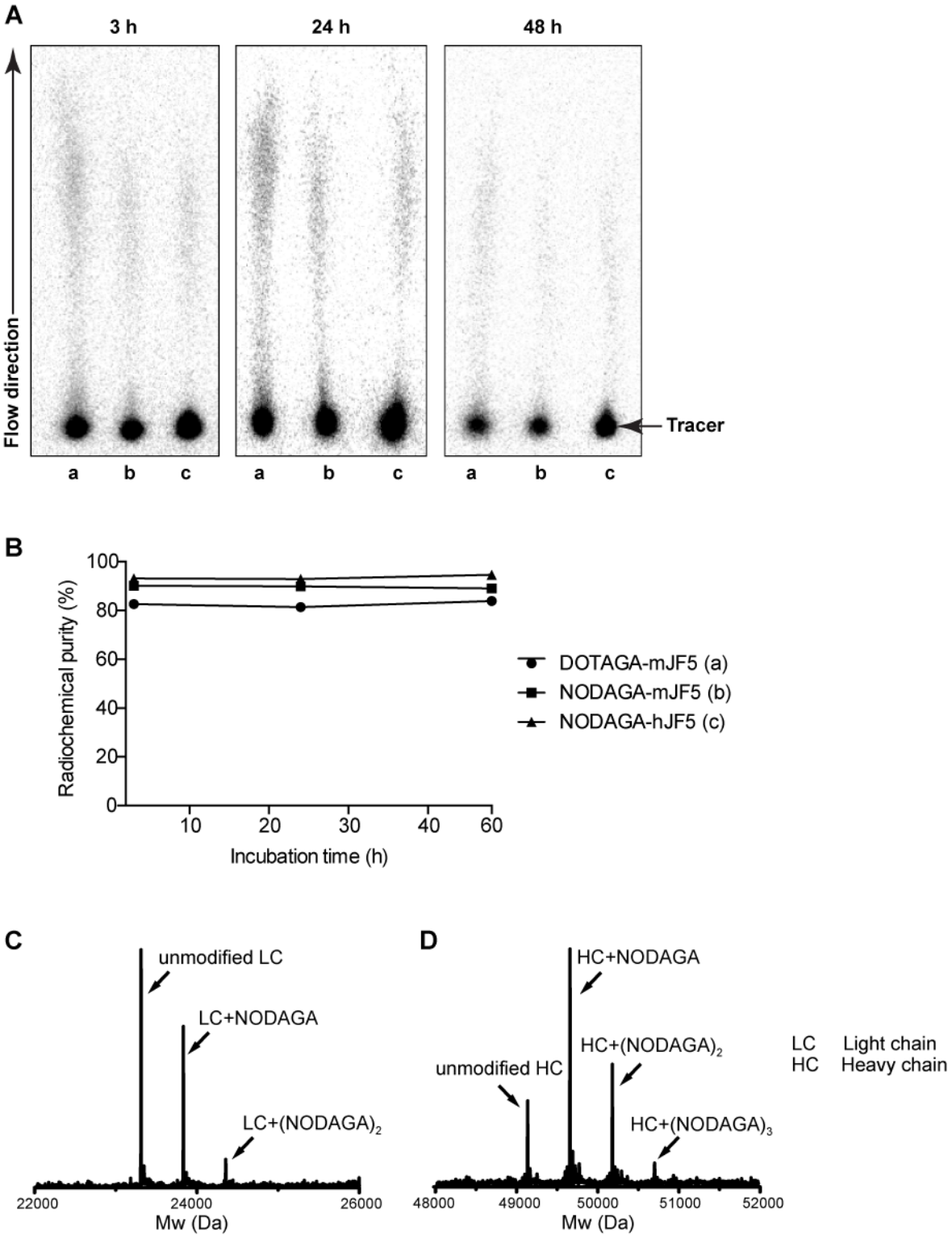

Supplementary Figure 3. A. Serum stability of the ^{64}Cu-labeled, chelator-conjugated hJF5 and mJF5 determined by TLC. Samples were run on iTLC-SG paper and then analyzed by autoradiography. a = DOTAGA-mJF5, b = NODAGA-mJF5, c = NODAGA-hJF5. Arrow = direction of flow. **B.** Serum stability of the ^{64}Cu-labelled, chelator-conjugated hJF5 and

mJF5. The radiochemical purity over the time of 48 h shows no signs of proteolytic degradations, protein aggregations or copper transchelations to serum proteins. **C** and **D**. Conjugation of NODAGA-NCS to hJF5 analyzed by LC-MS-ESI (DTT was used to separate the light from the heavy chain). Representative de-convoluted LC-MS spectra of the hJF5 light chain (**C**) and heavy chain (**D**), with up to two and three NODAGA chelators being conjugated, respectively. From the peak intensities, a conjugation ratio of approximately three was estimated.

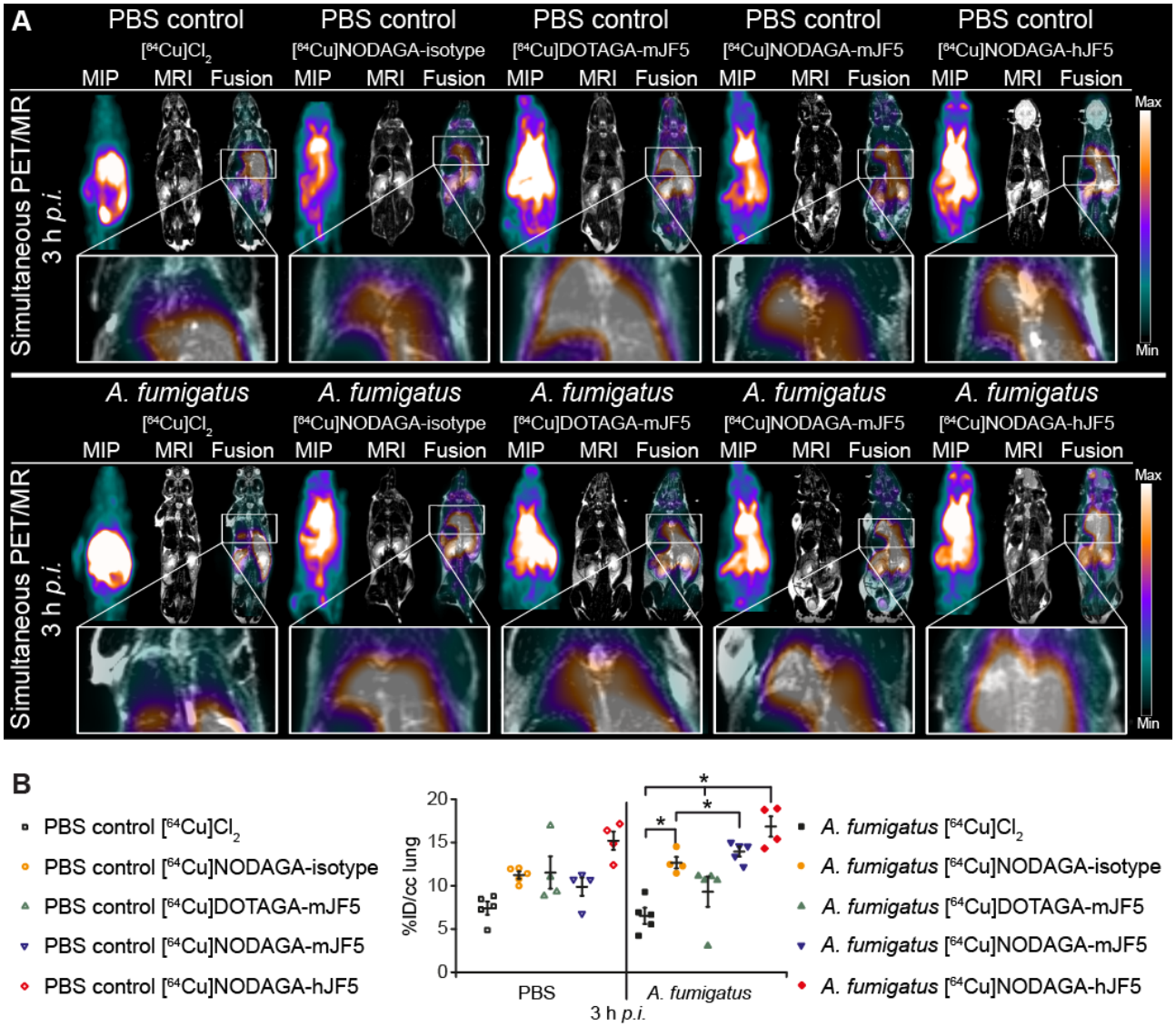

Supplementary Figure 4. A. *In vivo* biodistribution of [^{64}Cu]Cl_2, [^{64}Cu]NODAGA-isotype control, [^{64}Cu]DOTAGA-mJF5, [^{64}Cu]NODAGA-mJF5 and [^{64}Cu]NODAGA-hJF5 in PET/MR imaging at 3 h *p.i.* Coronal MIP, MR and fused PET/MR images of PBS treated mice and *A. fumigatus* infected mice injected with the respective tracers. **B.** Quantification of the *in vivo* PET insert images for the lung at 3 h *p.i.* in groups of n=4-5 mice. The graph shows the uptake of the various tracers in the lungs of infected animals and PBS controls at 3 h *p.i.* The quantification reveals higher tracer uptake in the lungs of animals injected with [^{64}Cu]NODAGA-hJF5 and lower tracer uptake in lungs of animals which received

[^{64}Cu]Cl_2. Data are expressed as the mean ± SD %ID/cc. Group differences were examined using one-way ANOVA, followed by post hoc Tukey–Kramer, *$P < 0.05$.

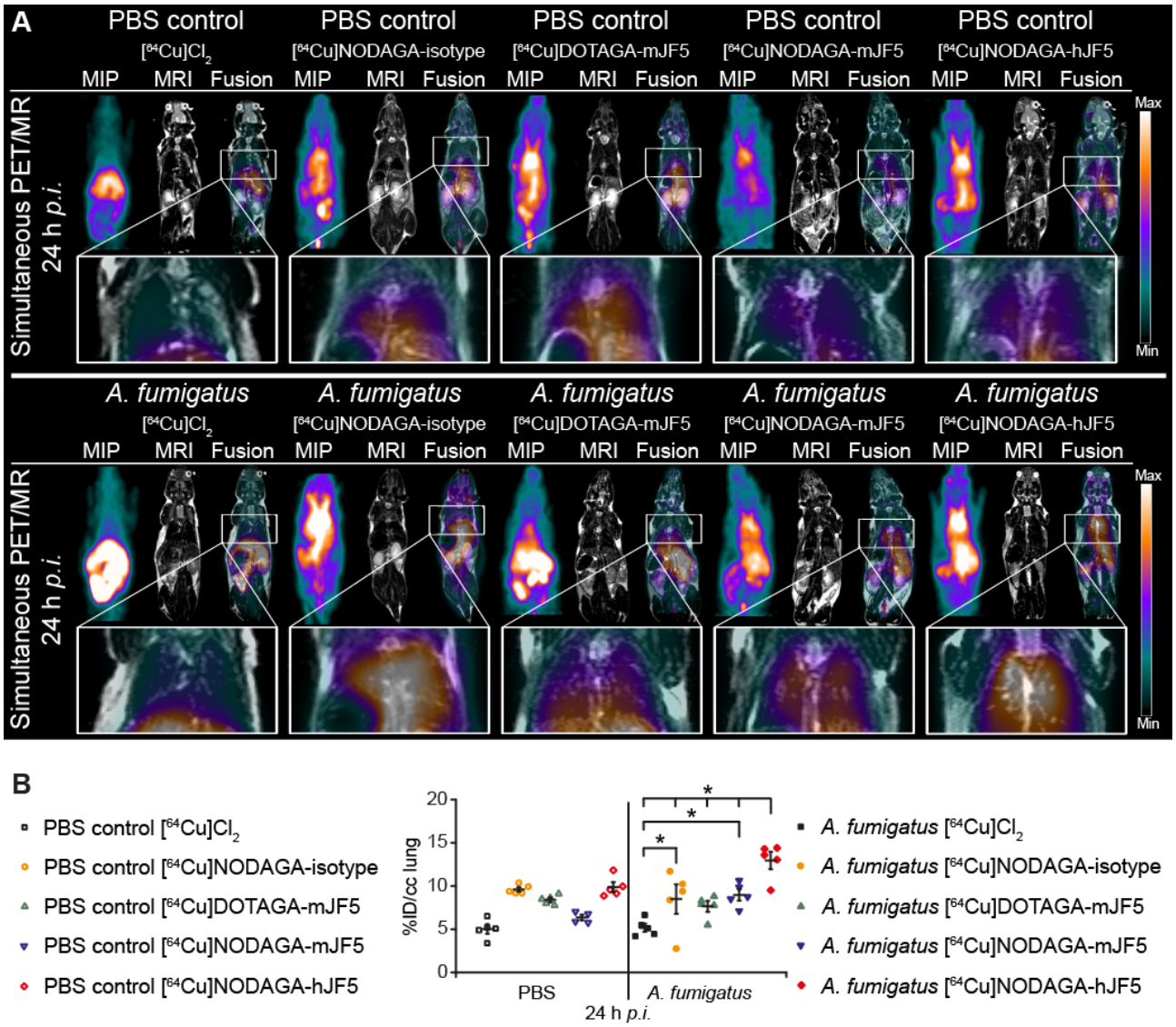

Supplementary Figure 5. A. *In vivo* biodistribution of [^{64}Cu]Cl_2, [^{64}Cu]NODAGA-isotype control, [^{64}Cu]DOTAGA-mJF5, [^{64}Cu]NODAGA-mJF5 and [^{64}Cu]NODAGA-hJF5 in PET/MR imaging at 24 h *p.i.* Coronal MIP, MR and fused PET/MR images of PBS treated mice and *A. fumigatus* infected mice injected with the respective tracers. The acquired images reveal the low lung uptake of [^{64}Cu]Cl_2 in both infected and PBS treated mice, affirming the specificity of the ^{64}Cu-labeled, chelator conjugated JF5 antibody tracers as it

excludes perfusion effects derived from infection-related inflammation. The image further displays the specific and high lung uptake of the chelator-conjugated antibody-based tracers in infected animals compared to the PBS treated control groups. Additionally, the MR image of infected animals shows the beginning of hyphal growth of *A. fumigatus* in the lung (hyperintense structures). **B.** Quantification (n=4-5 mice) of the *in vivo* PET insert images for the lung 24 h *p.i.* The graph shows the uptake of the different tracers in the lungs of infected animals and the PBS controls at 24 h *p.i.* Lower uptake was observed in the lungs of infected and PBS treated animals receiving [^{64}Cu]Cl_2. Infected mice which received the [^{64}Cu]NODAGA-hJF5 tracer show significantly higher lung uptakes compared to infected animals injected with [^{64}Cu]DOTAGA-mJF5, [^{64}Cu]NODAGA-mJF5 or [^{64}Cu]Cl_2 Data are expressed as the mean ± SD %ID/cc. Group differences were examined using one-way ANOVA, followed by post hoc Tukey–Kramer, *$P < 0.05$.

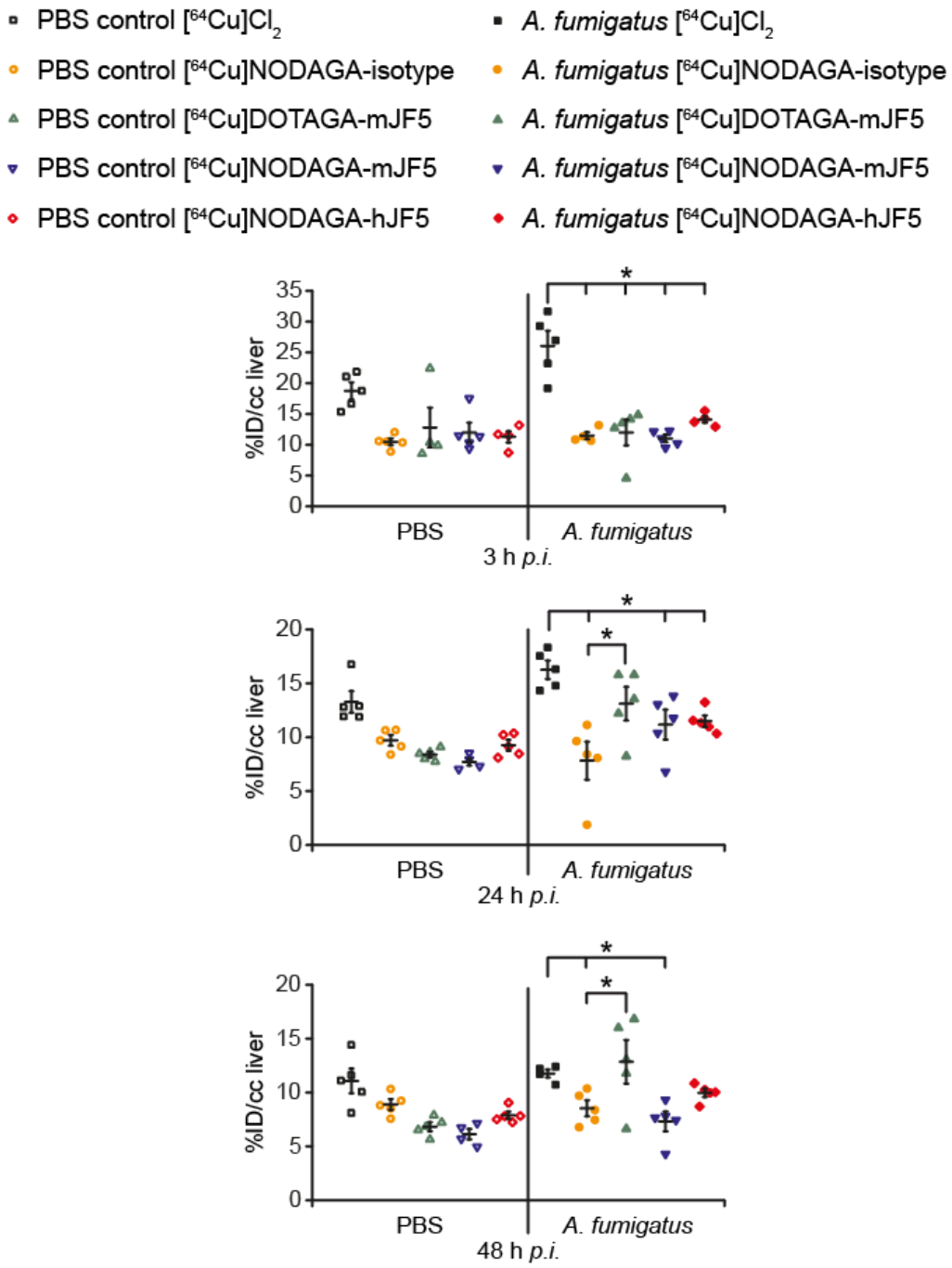

Supplementary Figure 6. Quantification of the *in vivo* PET insert data for the liver (n=4-5) at 3, 24 and 48 h *p.i.* The graphs display the uptake of the different antibody-based PET tracers in the liver of *A. fumigatus* infected and PBS treated control animals in groups of n=5 mice. Higher uptake of [^{64}Cu]Cl_2 is observed in healthy and infected animals 3 h *p.i.*

suggesting fast clearance of ^{64}Cu by the liver. Also, DOTAGA-conjugated mJF5 revealed higher uptake in the liver of *A. fumigatus* infected animals compared to the NODAGA-labeled antibodies 48 h *p.i.* Data are expressed as the mean ± SD %ID/cc. Group differences were examined using one-way ANOVA, followed by post hoc Tukey–Kramer, $*P < 0.05$.